Numerical Optimization of Large Shade Sail Support

Jakub Javorik
Faculty of Technology, Tomas Bata University in Zlín, Vavrečkova 275, 762 72 Zlín, Czech Republic. E-mail: javorik@ft.utb.cz

To design an optimal support of a large shade sail it is necessary to determine forces in wire ropes that support the sail. Relations between a sail loading and ropes reaction forces, rope diameters and sail stresses were investigated. To simulate the sail behavior and set up these relations, numerical (FEM) models were created and analyzed. Most of the results show nonlinear relations between above mentioned parameters and they depend on the sail geometry, applied loads and the rope diameter. It means that for every specific geometry and loading of particular sail an optimal rope diameter and support should be designed. The nonlinear numerical analysis is very suitable tool for this purpose and thus specialized systems based on the Finite Element Method (FEM) should be used to simulate and analyze such problems.

Keywords: Awnings, Numerical Model, Sail, Shade Sail, Wire Rope

1 Introduction

There are some applications where products of elastomer-coated fabric are used. They are often used as awnings, canopies, shade sails, light structures etc. [1-3] (Fig. 1). If they are used as shade sails, they are often designed with large dimensions. In such cases, we must consider significant loading of the sails due to weather influence such as a wind or a snow. Therefore an important task is to design the sail support appropriately [4-7].

Wire ropes are used as the support of the sail that is stretched between them. Our goal was to find out appropriate rope i.e. rope diameter for particular sail and set up relation between the sail load and the appropriate wire rope diameter.

We decided to create a numerical model of the sail supported by the wire ropes. Finite element method (FEM) was used to analyze the model and to design the ropes for the sails [8-11].

Fig. 1 *Application of Shading Sails [12]*

2 Material

2.1 Sail

The sails are made of a polyester fabric coated with a covering layer of an elastomer [13]. In terms of the mechanical properties, this material can be considered as in plane (2D) orthotropic. Therefore a material model that will be used for this material will be 2D orthotropic model with a linear stress-strain relationship (i.e. Hooke's law).

It is necessary to determine four material constants for the 2D orthotropic material model: 2 modules of elasticity (E_x – in the direction of the warp of the fabric, E_y – in the direction of the weft), Poisson ratio in the sail plane (ν_{xy}) and a shear modulus in the sail plane (G_{xy}). Basic axes of the material are set up according to the orientation of the fabric fibers. Warp direction will be defined as the x-axis, and the weft direction as the y-axis. The material constants were determined in laboratory tests and they are summarized in the Tab. 1.

Tab. 1 *Material Constants of Sail*

Constant	**Value**
Modulus of elasticity E_x	1 350 MPa
Modulus of elasticity E_y	1 100 MPa
Poisson ratio v_{xy}	0.235
Shear modulus G_{xy}	540 MPa
Warp strength R_x	98 MPa
Weft strength R_y	95 MPa

2.2 Wire Rope

In the model, the rope is created as an element having very low bending stiffness (which is given by its geometry) with following isotropic material characteristics that correspond to common wire ropes properties:

Modulus of elasticity: 90 000 MPa

Poisson ratio: 0.3

Analyses were performed for different diameters of the ropes. The rope diameters of commonly produced ropes were used, they are: 8, 9.5, 11.5, 19 and 22 mm. The safe load in Tab. 2 was computed from the minimum breaking strength through a safety factor s_f=5 [14].

Tab. 2 *Strength and Safe Load of Various Wire Ropes*

Rope Diameter [mm]	**Minimum Breaking Strength** [kN]	**Safe Load** [kN]
8.0	37.9	7.6
9.5	54.3	10.9
11.5	73.6	14.7
19.0	212.0	42.3
22.0	286.0	57.6

3 Method

3.1 Geometry of Numerical (FEM) Model

The sail is square shaped with a side length of 10 m. The square sides are not straight but have an arc shape with the arc height of 1 m (Fig. 2). Further, the corners are cut as shown in Fig. 3. The sail thickness is 0.446 mm.

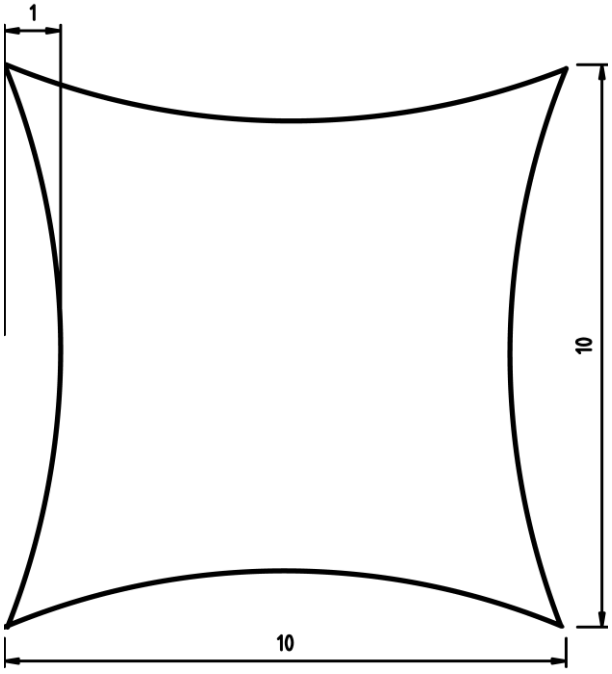

Fig. 2 *Sail Geometry (dimensions are in meters)*

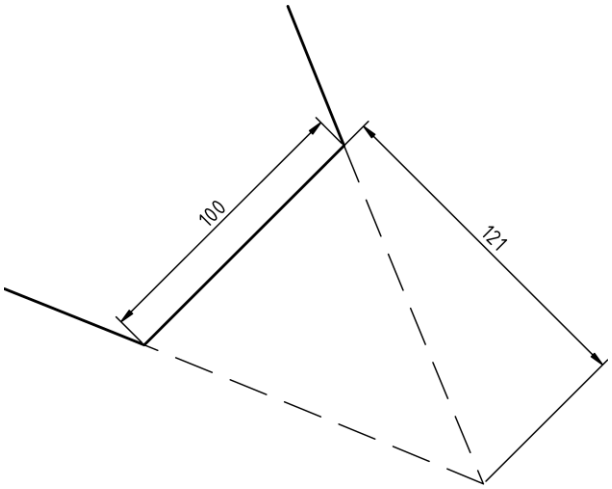

Fig. 3 *Detail of Sail Corner (dimensions are in millimeters)*

With regard to the symmetry of the sail shape and the symmetry of the boundary conditions, only a quarter model of sail was created for the analysis. Axes of the symmetry coincide with the diagonals of the sail (Fig. 4).

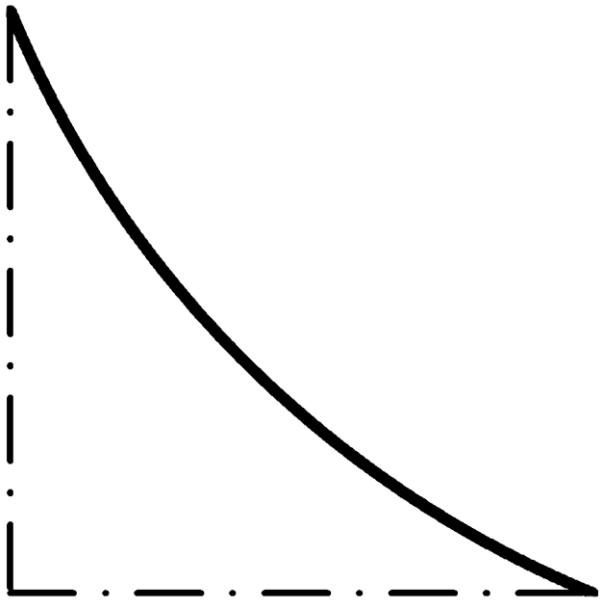

Fig. 4 *Quarter model of the sail*

3.2 Numerical Model

Based on the geometry described above, a finite element model was created. It consists of two types of finite elements. The sail is created from *shell* elements. The rope is made of 1D *beam* elements. The beam elements (rope) are placed on the edge of the sail, and they continue to the corners (Fig. 5). The beam elements are fixed at the edges with the shell elements. *X*-axis indicates the warp direction and *y*-axis indicates the weft direction in the Fig. 5.

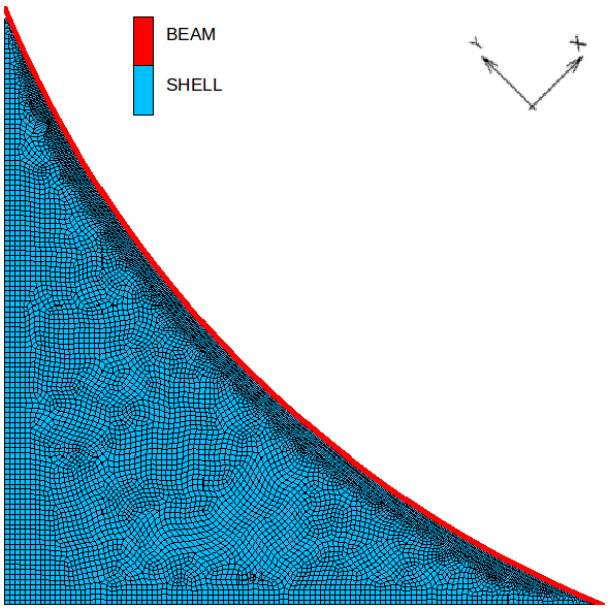

Fig. 5 *Elements of FEM Model of Sail*

Boundary conditions were defined to simulate the symmetry of the model and a load caused by different weather conditions. Primary, the quarter symmetry of the sail is defined. This symmetry is defined by removing the appropriate degrees of freedom (DOF) in the symmetry planes (i.e. on the sail diagonals). On the green diagonal (in Fig. 6) the displacement in the *x*-axis and rotation in axes *y*-and *z* were removed. On the yellow diagonal (in Fig. 6) the displacement in the *y*-axis and rotation in axes *x* and *z* were removed.

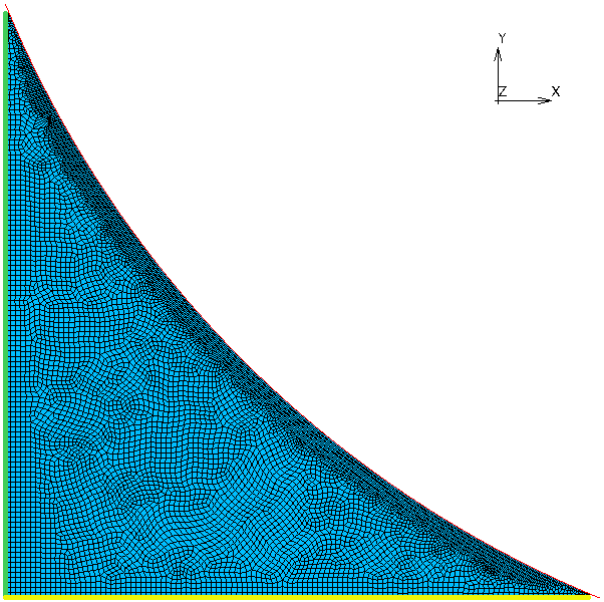

Fig. 6 *Boundary Conditions of Symmetry in Model*

The loading of the model was done in three steps. In the first step the rope is tensioned and the sail is stretched. In the second step a weight of the sail and rope takes effect, and a surface load is applied on the sail in the third step. The value of stress in the stretched sail must be 1.5 MPa. It means we must apply an appropriate tension of rope in the first step so that after the second step the maximum stress in the sail will be 1.5 MPa. In the third step surface load up to 200 kg/m^2 was applied and we studied when the safe load of the sail or of the rope will be exceeded. The rope tension, in the first step, was applied by moving the rope ends, it means that the right lower end was moved horizontally (*x*-axis in Fig. 6) and the upper left end was moved vertically (*y*-axis in Fig. 6). Forces required to preload ropes of particular diameters are given in the results.

4 Results

The analysis shows that the safe load capacity of the sail (loaded uniformly over the entire area) is 50 kg/m^2. This is the point where the safe stress in the weft direction is exceeded. The value of the safe weft stress was obtained from the weft strength (Tab. 1) using the safety factor s_f=5. It means that the safe stress in the weft is 95/5=19 MPa. Safe stress in the warp is 98/5=19.6 MPa, but this value was not reached within the load of 50 kg/m^2.

The main aim is to find a smallest diameter of the rope, which is able to hold up the sail loaded with the determined safe load (50 kg/m^2). Next results are load capacities of the ropes with other diameters and values of reaction forces in these ropes during a loading of the sail.

The minimum rope diameter for the safe load of the sail is diameter of 19 mm. The analysis suggests that the safe load of this rope (19 mm), that is 42.3 kN (Tab. 2), will be exceeded by the sail load of 49 kg/m^2. Critical is therefore the rope, but critical load (49 kg/m^2) for this case is very close of the sail critical load (50 kg/m^2). The critical load for the next standard rope diameter (22 mm) is as high as 69 kg/m^2, and therefore in this case, the load capacity of the sail (50 kg/m^2) would be crucial. The dependence of the critical sail load on the rope diameter (i.e. safe carrying capacity of ropes) is shown in Tab. 3 and Fig. 7. But because we still use one sail, its own carrying capacity remains the same, i.e. 50 kg/m^2.

Tab. 3 *Safe Loads (Load Capacities) for the Different Ropes*

Rope Diameter [mm]	**Safe Load** [kg/m^2]
8.0	8
9.5	10
11.5	13
19.0	49
22.0	69

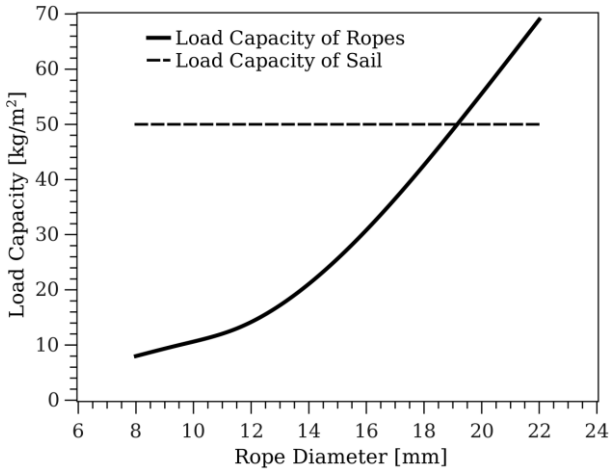

Fig. 7 *Relation between Rope Diameter and Load Capacity of Ropes*

Fig. 8 shows a change of the rope axial force i.e. the reaction force at the rope ends during the whole analysis. This graph is for the rope with the diameter of 19 mm. It is necessary to design the ropes supports according these values. The preload of ropes, in order to initially stretch the sail, is applied in the first time step (time 0 to1). Then the weight of the sail and the rope acts during the second time step. And the surface load, up to a final value of 49 kg/m^2, is applied finally in the third time step. The limit of rope safe load (42.3 kN) is reached at the end of this step.

In Fig. 9 a relation of the reaction rope force versus the sail load up to 200 kg/m^2 (only the third time step of analysis) can be seen. We can see the relation in a wide range of loading, far after the safe load was exceeded, but still below the values of the real rope or sail strengths, which are five times higher than the safe limits. It is evident that this relation is strongly nonlinear and thus it is not possible to design the ropes supports for other sail shapes and dimensions simply by linear relations. New nonlinear numerical analyses would be necessary in the case of a different sails geometry and dimensions or rope diameters. Similarly (like in Fig. 9) Fig. 10 shows the dependence of the stress in the sail on the load.

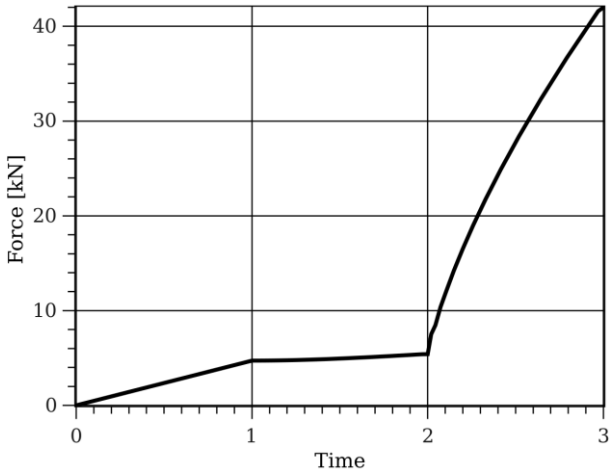

Fig. 8 *Rope Axial Force Change during Loading*

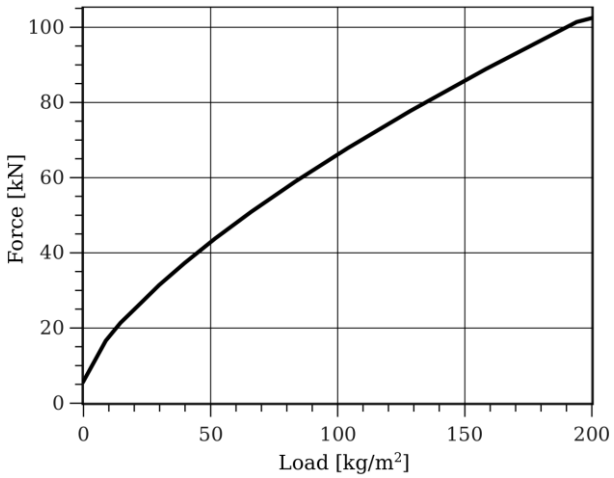

Fig. 9 *Relation between Sail Load and Rope Axial Force (in 3rd time step of analysis)*

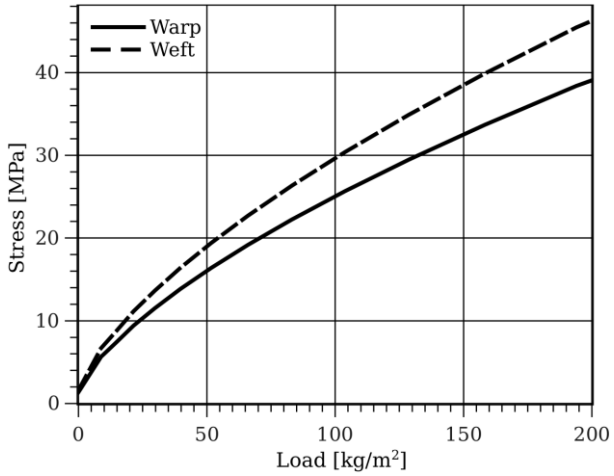

Fig. 10 *Relation between Sail Load and Stress in Sail (in 3rd time step of the analysis)*

Finally the force required for the initial preload of the sail, which is achieved on the end of the second time step (including the effect of the weight of the rope and the sail) are presented in Tab. 4 and in Fig. 11. The initial preload occurs when the middle value of stress between warp and weft reaches value of 1.5 MPa.

Tab. 4 *Preload for Different Ropes*

Rope Diameter [mm]	**Preload Force** [kN]
8.0	1.4
9.5	2.4
11.5	4.0
19.0	5.8
22.0	6.3

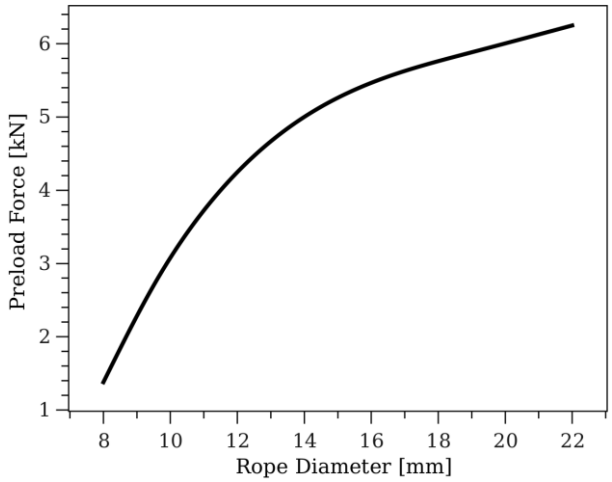

Fig. 11 *Dependence of Preload Force on Rope Diameter (end of 2nd time step of analysis)*

5 Summary

To design the shade sails it is necessary to determine the actual carrying capacity of the particular sail firstly. This capacity is given mainly by the sail material, its geometry and boundary conditions. The calculated carrying capacity of the sail is then used to design the appropriate diameter of the supporting wire rope.

For the 10x10m square sail with the side-arc high 1m safe carrying capacity of 50 kg/m^2 was calculated. Such sail should be supported by the wire rope with the diameter of 19 mm. The numerical analysis showed that this rope is able safely supports the sail up to load of 49 kg/m^2.

Models with different rope diameters were analyzed and we found out that the relation between such parameters as the sail loading, stress in the sail, axial force in the rope and rope diameter are strongly nonlinear. These facts mean that we can not use simple linear relations to design the sail supports, but for different sail geometry, material, loads etc. we must use appropriate nonlinear numerical analysis.

References

[1] JUANICÓ, L. E., (2009). A new design of configurable solar awning for managing cooling and heating loads. In: *Energy and Buildings*. Vol. 41, No. 12, pp. 1381 – 1385. Elsevier BV.

[2] BRODERICK, R., (2003). The arts of fabric. In: *Fabric Architecture*. Vol. 15, No. 2, pp. 46 – 50. Industrial Fabrics Association International. Minnesota.

[3] EILAM, I., (2006). An awning on every home. In: *Industrial Fabric Products Review*. Vol. 91, No. 4, pp. 20 – 26. Industrial Fabrics Association International. Minnesota.

[4] YIMIN, L., JIE, W. (2014). Design and calculation of multi-angel and stepping transmission of sucker rod forging. In: *Manufacturing Technology*. Vol. 14, No. 4, pp. 650 – 657. Univerzita J. E. Purkyne. Czech Republic.

[5] RUSNAKOVA, S., FOJTL, L., ZALUDEK, M., RUSNAK, V. (2014). Design of material composition and technology verification for composite front end cabs. In: *Manufacturing Technology*. Vol. 14, No. 4, pp. 607 – 611. Univerzita J. E. Purkyne. Czech Republic.

[6] JAVORIK, J. (2014) Simulation and Numerical Analysis of Pneumatic Actuator Behavior. In: *International Journal of Mathematics and Computers in Simulation*. Vol. 8, No. 1, pp. 189 – 196. North Atlantic University Union. Oregon.

[7] SAMEK, D., JAVORIK, J. (2013) Numerical analysis of shape stability of rubber boot. In: *International Journal of Mechanics*. Vol. 7, No. 1, pp. 293 – 301. North Atlantic University Union. Oregon.

[8] ŽMINDÁK, M., MĚŠKO, J., PELAGIČ, Z., ZRAK, A. (2014). Finite element analysis of crack growth in pipelines. In: *Manufacturing Technology*. Vol. 14, No. 1, pp. 116 – 122. Univerzita J. E. Purkyne. Czech Republic.

[9] DELYOVÁ, I., HRONCOVÁ, D., FRANKOVSKÝ, P. (2014). Analysis of simple mechanism using MSC Adams. In: *Manufacturing Technology*. Vol. 14, No. 2, pp. 141 – 145. Univerzita J. E. Purkyne. Czech Republic.

[10] JAVORIK, J., BILEK, O. (2014). Numerical analysis of bushing of car stabilizer. In: *International Journal of Mechanics*. Vol. 8, No. 1, pp. 289 – 297. North Atlantic University Union. Oregon.

[11] JAVORIK, J., STANEK, M. (2011). The shape optimization of the pneumatic valve diaphragms. In: *International Journal of Mathematics and Computers in Simulation.* Vol. 5, No. 4, pp. 361 – 369. North Atlantic University Union. Oregon.

[12] Creative Commons licensed picture *Blue aerodynamic modern awnings* from author Wonderlane is available at https://www.flickr.com/photos/wonderlane/4648749377/in/photostream/ and is licensed under the CC BY 2.0 license, terms and conditions are available at https://creativecommons.org/licenses/by/2.0/.

[13] TAYYAR, A. E., ALAN, G. (2015). Outdoor usage performances of woven fabrics dyed with self-cleaning dyes. In: *Journal of the Textile Institute*. Vol. 106, No. 3, pp. 303 – 310. Taylor and Francis Ltd.

[14] FEYRER, K. (2007). *Wire Ropes, Tension, Endurance, Reliability*. Springer, Berlin, Heidelberg, New York.